A geometric singular perturbation analysis of generalised shock selection rules in reaction-nonlinear diffusion models

Bronwyn Bradshaw-Hajek[1], Ian Lizarraga[2], Robert Marangell[2], and Martin Wechselberger[2]

[1]UniSA STEM, University of South Australia, Mawson Lakes, South Australia, Australia
[2]School of Mathematics and Statistics, University of Sydney, NSW, Australia

Abstract

Reaction-nonlinear diffusion (RND) partial differential equations are a fruitful playground to model the formation of sharp travelling fronts, a fundamental pattern in nature. In this work, we demonstrate the utility and scope of regularisation as a technique to investigate shock-fronted solutions of RND PDEs, using geometric singular perturbation theory (GSPT) as the mathematical framework. In particular, we show that *composite* regularisations can be used to construct families of shock-fronted travelling waves sweeping out distinct generalised area rules, which interpolate between the equal area and extremal area (i.e. algebraic decay) rules that are well-known in the shockwave literature. Our analysis blends Melnikov methods with GSPT techniques applied to the PDE over distinct spatiotemporal scales.

We also consider the spectral stability of these new interpolated shockwaves. Using techniques from geometric spectral stability theory, we determine that our RND PDE admits nonlinearly stable shock-fronted travelling waves. The multiple-scale nature of the regularised RND PDE continues to play an important role in the analysis of the spectral problem.

1 Motivation

Wave fronts are ubiquitous in nature. In the context of population dynamics, such waves may represent patterns or structure in migrating populations. Reaction-diffusion equations, such as the extensively studied Fisher equation [6], are used to model population growth dynamics combined with a simple Fickian diffusion process, and are typically capable of exhibiting travelling wave solutions.

In cell migration, advection (or transport) is another important model mechanism. It may represent, e.g., tactically-driven movement, where cells migrate in a directed manner in response to a concentration gradient. Such a concentration gradient develops, for example, in a soluble fluid (chemotaxis) or as a gradient of cellular adhesion sites or of substrate-bound chemoattractants (haptotaxis). Well studied examples of individual cells exhibiting directed motion in response to a chemical gradient include bacteria chemotactically migrating towards a food source. Wound healing, angiogenesis or malignant tumor invasion are just a few examples of chemotactic and/or haptotactic cell movement where the migrating cells form part of a dense population of cells as may be found in tissues. Such migrating cell populations not only form travelling waves but may

also develop sharp interfaces in the wave form.

From a classical PDE point of view, these advection-reaction models may represent hyperbolic balance laws (hyperbolic conservation laws with source terms), and the formation of shock fronts is well known. In general, shocks are problematic because as the wave front steepens (and a shock forms) the solution becomes multivalued and physically nonsensical. The model breaks down and it becomes impossible to compute the temporal evolution of the solution [18].

To account for shocks, modellers have employed the technique of *regularisation* – adding small higher order terms to these models to smooth out the shocks. In the context of hyperbolic conservation/balance laws, these are usually small viscous (diffusive) regularisations, e.g., the viscous Burgers equation. Due to dissipative mechanisms, these physical shocks are observed as narrow transition regions with steep gradients of field variables. Mathematically, questions of existence and uniqueness of such viscous shock profiles are fundamental.[1]

Another source for the formation of sharp interfaces can be found in density-dependent nonlinear diffusion processes. Through sensing the local cell density, cells make informed decisions, i.e., they perform a 'biased walk'. This could lead to, e.g., the tendency to cluster or aggregate with other nearby cells; think of flocking or swarming, which might develop as an evolutionary advantage for the cell population. Such aggregation mechanisms can be achieved through, e.g., negative (or backward) diffusion. Such reaction-nonlinear diffusion (RND) models may form shocks. Again, modellers have employed the technique of *regularisation* – adding small higher order terms to these models to 'smooth' the shocks, but these are not so well-known, at least in the bioscientific community. Possible shock formation in such regularised RND models is the main focus of this presentation, and we will use tools from geometric singular perturbation theory and dynamical systems theory to tackle this problem.

2 The setup for RND Models

We start by considering a dimensionless reaction–nonlinear diffusion model of the form

$$u_t = (D(u)u_x)_x + f(u) = \Phi(u)_{xx} + f(u) \tag{1}$$

where $x \in \mathbb{R}$ denotes the spatial domain, $t \in \mathbb{R}_+$ denotes the time domain, $u \in \mathbb{R}_+$ denotes a (population/agent) density, $D(u)$ models a (population/agent) density dependent diffusivity. $\Phi(u)$ is an anti-derivative of $D(u)$, i.e. $\Phi'(u) = D(u)$, referred to as the *potential*. The (dimensionless) population/agent density u is scaled such that $u \in [0, 1]$ forms the domain of interest where $u = 1$ is the carrying capacity of the population/agent density. This domain of interest is also reflected in the reaction term $f(u)$ which is modelled either as *logistic growth* or as *bistable growth*. We consider the latter in this paper:

$$f(u) = \kappa u(u - \alpha)(1 - u)\,,\ \kappa > 0,\ 0 < \alpha < 1.$$

We focus on RND models where not only diffusion is present but also *aggregation* (or *backward diffusion*) [3, 10, 5, 19, 20]. The heuristic motivation for this modelling assumption is based on

[1] Another option is dispersive regularisation, e.g., the KdV equation. Note that both regularisations (viscous and dispersive) deal with the same equation (inviscid Burgers) but create very different outcomes.

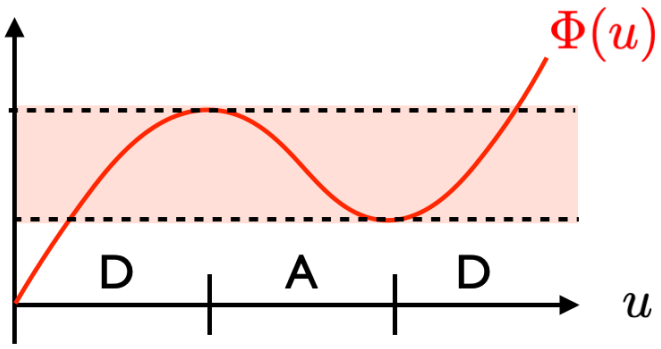

Figure 1: The graph of the potential and admissible jump zone (shaded) that allows for possible shock connections. We denote the graph $(u, \Phi(u))$ by $S = S_s^l \cup F_l \cup S_m \cup F_r \cup S_s^r$ which is referred to as a critical manifold; see section 3 for details. Possible shocks are confined to a fixed potential value $\Phi(u) = const$, i.e. jumps must occur over the middle branch of the potential, S_m, connecting the outer two branches of the potential, S_s^r and S_s^l (shaded region).

the observation that populations tend to cluster for, e.g., safety (to avoid easy predation). By imposing different motility rates for agents that are isolated compared to other agents, one obtains density dependent nonlinear diffusion [11]. Aggregation will manifest itself in these models in sign changes of the density dependent diffusion coefficient $D(u)$. The simplest density-dependent nonlinear diffusion coefficient model that we consider is of the polynomial form

$$D(u) = \beta(u - \gamma_1)(u - \gamma_2) \tag{2}$$

with $0 < \gamma_1 < \gamma_2 < 1$, i.e., diffusion-aggregation-diffusion (DAD) in the domain of interest. For sparse population density diffusive behaviour is assumed, while for intermediate population density aggregation will happen which again turns into diffusive behaviour for large population densities (close to carrying capacity).

2.1 Shock fronts in the RND model (1)

Shock formation is a well-known phenomenon in the case of a nonlinear advection-reaction model which defines a hyperbolic balance law (under certain assumptions). Similarly, nonlinear diffusitivity $D(u)$ including a domain with negative diffusitivity can also cause shock formation in an RND model [5, 21, 22]. Here, we focus on the DAD case throughout this document. A corresponding 'cubic' potential Φ is sketched in Figure 1.

Let us look for one of the simplest possible coherent structures in such RND models (1), travelling waves with wave speed $c \in \mathbb{R}$ that connect the asymptotic end states $u_- = 1 \to u_+ = 0$ or vice versa, i.e., population/agents invade or evade the unoccupied domain with constant speed. A travelling wave analysis introduces a co-moving frame $z = x - ct$ in (1), $c \in \mathbb{R}$. Stationary solutions, i.e., $u_t = 0$, in this co-moving frame include travelling waves/fronts, and they are found as special (heteroclinic) solutions of the corresponding ODE problem

$$-cu_z - (D(u)u_z)_z = f(u)\,.$$

Define $v := -cu - D(u)u_z$ to obtain the corresponding 2D dynamical system

$$\begin{aligned} D(u)u_z &= -(v + cu) \\ v_z &= f(u)\,. \end{aligned} \tag{3}$$

Note that this dynamical system is singular where $D(u) = 0$, i.e., wherever the diffusion-aggregation transition happens. To be able to study this problem (3) on the whole domain of interest including these transition zones near $D(u) = 0$, we make an auxiliary state-dependent transformation $dz = D(u)d\zeta$ which gives the so-called *desingularised problem*

$$\begin{aligned} u_\zeta &= -(v + cu) \\ v_\zeta &= D(u)f(u)\,. \end{aligned} \tag{4}$$

This problem is topologically equivalent to (3) in the diffusion regime $D(u) > 0$ while one has to reverse the orientation in the aggregation regime $D(u) < 0$ to obtain the equivalent flow. We classify all singularities of (3) by analysing the auxiliary system, the desingularised problem (4).

Remark 2.1 *We emphasize that the auxiliary system is only a proxy system to study the problem near $D(u) = 0$. To completely understand the original flow near $D(u) = 0$, one has to use additional techniques such as the blow-up method; see, e.g., [23].*

The asymptotic end states of the travelling waves form equilibrium states of the desingularised (and the original) problem defined by $f(u_\pm) = 0$, and $v_\pm = -cu_\pm$. Our focus is on these asymptotic end states given by the equilibria

$$(u_\mp, v_\mp) = (1, -c)\,, \qquad (u_\pm, v_\pm) = (0, 0)$$

$D(u)$	$f(u)$	$(u_\mp, v_\mp)$	$(u_\pm, v_\pm)$
DAD	logistic/bistable	S_s^r	S_s^l

Table 1: Location of asymptotic end states on critical manifold S

In the case of a bistable reaction term, there exists an additional equilibrium in the domain of interest defined by $f(u_b = \alpha) = 0$ which gives $(u_b, v_b) = (\alpha, -c\alpha)$. This extra equilibrium is located as follows:

$D(u)$	$f(u)$	$\alpha > \gamma_2$	$\gamma_1 < \alpha < \gamma_2$	$\alpha < \gamma_1$
DAD	bistable	S_s^r	S_m	S_s^l

Table 2: Location of additional equilibrium (u_b, v_b) on critical manifold S in the bistable case

The Jacobian evaluated at any of these equilibria $(u_{\pm,b}, v_{\pm,b})$ is given by

$$J = \begin{pmatrix} -c & -1 \\ D(u_{\pm,b})f'(u_{\pm,b}) & 0 \end{pmatrix}$$

which has $\operatorname{tr} J = -c$ and $\det J = D(u_{\pm,b})f'(u_{\pm,b})$. The types of equilibria are summarized in the following table.

$D(u)$	$f(u)$	(u_-, v_-)	(u_+, v_+)	(u_b, v_b), $\alpha > \gamma_2$	(u_b, v_b), $\gamma_1 < \alpha < \gamma_2$	(u_b, v_b), $\alpha < \gamma_1$
DAD	logistic	Saddle	(un)stable NF	-	-	-
DAD	bistable	Saddle	Saddle	(un)stable NF	Saddle	(un)stable NF

Table 3: Type of equilibria on critical manifold S

The distinction between Node and Focus (NF) depends on the sign of the discriminant

$$\mathcal{D} := c^2 - 4D(u_{\pm,b})f'(u_{\pm,b})\,,$$

$\mathcal{D} > 0$ (Node) or $\mathcal{D} < 0$ (Focus). The distinction between stable $c > 0$ and unstable $c < 0$ depends on the sign of the wave speed.[2]

Remark 2.2 *The desingularised system* (4) *defines another type of singularities for the original problem through* $D(u) = 0$ *which are known as* folded singularities*; see, e.g., [26]. These will be discussed in more detail in section (cite).*

We are interested in a travelling front/wave in this system corresponding to a heteroclinic connection from one steady state ($u_\mp = 1$) to the other ($u_\pm = 0$) or vice versa.
In our setup of the RND model, such a solution (if it exists) cannot be smooth, because the zeros of the diffusion coefficient $D(u)$ which exist in the relevant domain of interest $u \in [0, 1]$ define singularities in this problem. Discontinuous jumps (shocks) must be incorporated by studying *weak* solutions of the original PDE problem (1). Furthermore, nonunique families of shock-type weak solutions can be expected to coexist (Hollig), with the shock occurring anywhere within the admissible jump zone.

To handle these issues, we employ the technique of regularisation to our RND system (1) to obtain locally unique (smoothed) classical solutions of the PDE. In particular, we will show that weighted combinations of two distinct regularisations essentially allow us to select traveling waves obeying particular shock criteria from within the admissible jump zone.

2.2 Regularisations of RND models

Regularisation of RND models is typically considered in one of two ways [20, 21]. The first method of regularisation accounts for *viscous relaxation* by adding a small temporal change in the diffusivity:

$$u_t = (\Phi(u) + \varepsilon u_t)_{xx} + f(u), \qquad 0 \le \varepsilon \ll 1. \tag{5}$$

The second of these involves adding a small change in the potential to account for *nonlocal effects*, leading to:

$$u_t = (\Phi(u) - \varepsilon^2 u_{xx})_{xx} + f(u), \qquad 0 \le \varepsilon \ll 1. \tag{6}$$

These regularisation techniques have been widely employed in models of chemical phase-separation, though they have gone relatively unnoticed in biological models until very recently.

[2] In case of a standing wave, any NF becomes a centre.

Here, we study the possible effects of *both* regularisations in a single RND model, i.e.,

$$u_t = (\Phi(u) + \varepsilon a u_t - \varepsilon^2 u_{xx})_{xx} + f(u), \qquad 0 \leq \varepsilon \ll 1, a \geq 0. \tag{7}$$

Since we only consider small perturbative regularisations $0 < \varepsilon \ll 1$, these models are so-called *singularly perturbed systems* and, as a consequence, the powerful machinery of geometric singular perturbation theory (GSPT) is applicable [4, 12, 26], as we shall explain in this manuscript.

Remark 2.3 *This regularised RND model* (7) *can be derived from the history dependent energy functional*

$$E(u) = \int_\Omega \left(F(u) + \varepsilon a \int_0^t u_s^2 ds + \frac{\varepsilon^2}{2} |u_x|^2 \right) dx \,,$$

where $F(u) = \int \Phi(u) du$ *is the free energy density function of the homogeneous state. The interfacial energy,* $\frac{\varepsilon^2}{2}|u_x|^2$*, introduces smoothing effects in regions with large gradients, and so does the memory term,* $\varepsilon a \int_0^t u_s^2 ds$*, which can be interpreted as visco-elastic potential energy; see, e.g., [27].*

Remark 2.4 *Continuum macroscale models can also be derived from lattice-based microscale models; see [11] for leading order RND models and [2] for regularised RND models (albeit more complicated).*

3 Travelling wave analysis of the regularised RND model (7)

We derive conditions based on the specific functions $D(u)$ and $f(u)$ that lead to travelling waves with sharp interfaces (shocks) in one spatial dimension. We introduce a travelling wave coordinate $z = x - ct$ for waves with speed $c \in \mathbb{R}$ and ask for stationary states of the PDE in the transformed frame. This transforms the regularised RND model (7) into a fourth order ordinary differential equation

$$-c u_z = \Phi(u)_{zz} - \varepsilon a c u_{zzz} - \varepsilon^2 u_{zzzz} + f(u) \,, \tag{8}$$

which we can recast as a *singularly perturbed dynamical system* in standard form

$$\begin{aligned} \varepsilon u_z &= \hat{u} \\ \varepsilon \hat{u}_z &= w + \Phi(u) - \delta \hat{u} \\ v_z &= f(u) \\ w_z &= v + cu \,. \end{aligned} \tag{9}$$

where $(u, \hat{u}) \in \mathbb{R}^2$ are 'fast' variables, $(v, w) \in \mathbb{R}^2$ are 'slow' variables, $\varepsilon \ll 1$ is the singular perturbation parameter, and $\delta := ac$.

Rescaling the 'slow' independent travelling wave variable $dz = \varepsilon dy$ in (9) gives the equivalent fast system

$$\begin{aligned} u_y &= \hat{u} \\ \hat{u}_y &= w + \Phi(u) - \delta \hat{u} \\ v_y &= \varepsilon f(u) \\ w_y &= \varepsilon (v + cu) \,. \end{aligned} \tag{10}$$

with the 'fast' independent travelling wave variable y. These equivalent dynamical systems (9) respectively (10) have a symmetry

$$(\hat{u}, v, c, y) \leftrightarrow (-\hat{u}, -v, -c, -y), \quad \text{resp.} \quad (\hat{u}, v, c, z) \leftrightarrow (-\hat{u}, -v, -c, -z)\,.$$

The aim is to use methods from GSPT to analyse the travelling wave problem in its 'slow' and 'fast' singular limit, and to obtain results on the existence (and stability) of travelling waves in the full regularised RND problem.

3.1 The limit on the 'fast' scale - the layer problem

We begin with the 'fast' system (10). Here the limit $\varepsilon \to 0$ gives the *layer problem*

$$\begin{aligned} u_y &= \hat{u} \\ \hat{u}_y &= w + \Phi(u) - \delta\hat{u} \\ v_y = w_y &= 0\,, \end{aligned} \tag{11}$$

i.e., (v, w) are considered parameters. Hence, the flow is along two-dimensional fast fibers $\mathcal{L} := \{(u, \hat{u}, v, w) \in \mathbb{R}^4 : (v, w) = const\}$. The set of equilibria of the layer problem,

$$S := \{(u, \hat{u}, v, w) \in \mathbb{R}^4 : \hat{u} = \hat{u}(u, v) = 0,\, w = w(u, v) = -\Phi(u)\}\,, \tag{12}$$

forms the two-dimensional *critical manifold* of the problem which is a graph over (u, v)-space. In the assumed diffusion-aggregation-diffusion (DAD) setup of (2), we have a sign change in the diffusivity along the one-dimensional set

$$F := \{(u, \hat{u}, v, w) \in S : D(u) = 0\}\,, \tag{13}$$

where $F = F_l \cup F_r = \{(u, \hat{u}, v, w) \in S : u = \gamma_1\} \cup \{(u, \hat{u}, v, w) \in S : u = \gamma_2\}$. Thus we have a splitting of the critical manifold $S = S_s^l \cup F_l \cup S_m \cup F_r \cup S_s^r$ where

$$\begin{aligned} S_s^l :=& \{(u, \hat{u}, v, w) \in \mathbb{R}^4 : \hat{u} = \hat{u}(u, v) = 0,\, w = w(u, v) = -\Phi(u),\, u < \gamma_1\} \\ S_s^r :=& \{(u, \hat{u}, v, w) \in \mathbb{R}^4 : \hat{u} = \hat{u}(u, v) = 0,\, w = w(u, v) = -\Phi(u),\, u > \gamma_2\} \\ S_m :=& \{(u, \hat{u}, v, w) \in \mathbb{R}^4 : \hat{u} = \hat{u}(u, v) = 0,\, w = w(u, v) = -\Phi(u),\, \gamma_1 < u < \gamma_2\}\,, \end{aligned}$$

see Figure 2.
The stability property of this set of equilibria S is determined by the two non-trivial eigenvalues of the layer problem, i.e., the eigenvalues of the Jacobian evaluated along S,

$$J = \begin{pmatrix} 0 & 1 \\ D(u) & -\delta \end{pmatrix}. \tag{14}$$

This matrix has $\mathrm{tr}J = -\delta$ and $\det J = -D(u)$. Hence, for $D(u) > 0$ the outer branches $S_s^{l/r}$ are normally-hyperbolic and of saddle-type (S-type). For $\delta \neq 0$ and $D(u) < 0$ the middle-branchS_m is also normally-hyperbolic, focus/node-type (FN-type), while for $\delta = 0$ and $D(u) < 0$ the middle-branch S_m loses normal-hyperbolicity and is of centre-type (C-type). Loss of normal hyperbolicity happens also along the one-dimensional sets $F = F_l \cup F_r$ where $\det J = 0$.

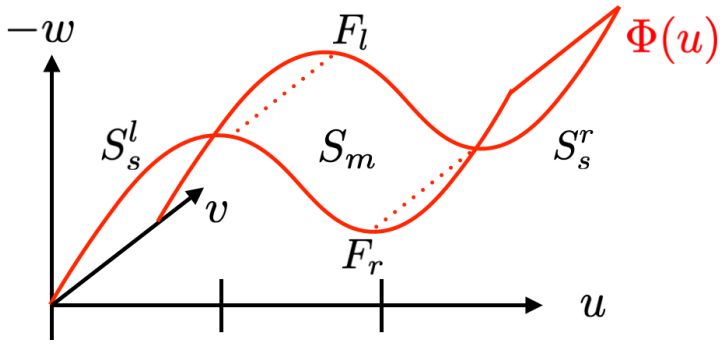

Figure 2: sketch of the two-dimensional critical manifold S projected onto (u, v, w)-space.

3.1.1 The $\delta = 0$ case

In this case, the layer problem (11),

$$\begin{aligned} u_y &= \hat{u} \\ \hat{u}_y &= w + \Phi(u) \end{aligned} \tag{15}$$

is Hamiltonian with

$$H(u, \hat{u}) = \frac{\hat{u}^2}{2} - \int (w + \Phi(u)) du \,. \tag{16}$$

Trajectories of this layer problem are confined to level sets of the Hamiltonian (16), i.e., $H(u, \hat{u}) = k$. Possible trajectories that are able to connect equilibrium points on different branches of the critical manifold S are confined to the saddle branches $S_s^{l/r}$ including the boundaries $F_{l/r}$. The corresponding equilibrium points $p_{l/r} = (u_{l/r}, 0, v_{l/r}, -\Phi(u_{l/r})) \in S_s^{l/r} \cup F_{l/r}$ of such connections must fulfill $v_l = v_r$ and $\Phi(u_l) = \Phi(u_r)$ since v and w are constant.

Remark 3.1 *This creates a bound on possible w-values, $w \in [-\Phi(u_{f-}), -\Phi(u_{f+})]$ where $D(u_{f\mp}) = 0$, i.e., confined to region between the local extrema of Φ.*

Without loss of generality, set $H(u_l, \hat{u} = 0) = 0$, i.e., $H(u, \hat{u}) = \frac{\hat{u}^2}{2} - \int_{u_l}^{u} (w + \Phi(u)) du$. Then $H(u_r, \hat{u} = 0)$ must be equal zero as well for the existence of a layer connection between these two points. This constraint leads to the well-known *'equal area rule'* (see, e.g. [21]),

$$\boxed{\int_{u_l}^{u_r} (w_h + \Phi(u)) du = 0} \,. \tag{17}$$

This rule allows for $S_s^{l/r}$ to $S_s^{r/l}$ connections, but not to the boundaries $F_{l/r}$ or the centre-type middle branch S_m. Due to the symmetry $(\hat{u} \leftrightarrow -\hat{u})$, there exists automatically a pair of such heteroclinic connections for fixed $w = w_h$, i.e., $\Gamma_+(w_h, 0) : p_l \to p_r$ and $\Gamma_-(w_h, 0) : p_r \to p_l$.

Remark 3.2 *The equal area rule* (17) *determines the value $w = w_h$ for which this integral vanishes. For $a = 0$, it is independent of the possible wave speed $c \in \mathbb{R}$. On the other hand, for $c = 0$ it is independent of the viscous relaxation regularisation component $a \in \mathbb{R}$. Hence, the only shock-fronted standing waves that our regularised model can produce are those satisfying the equal area rule.*

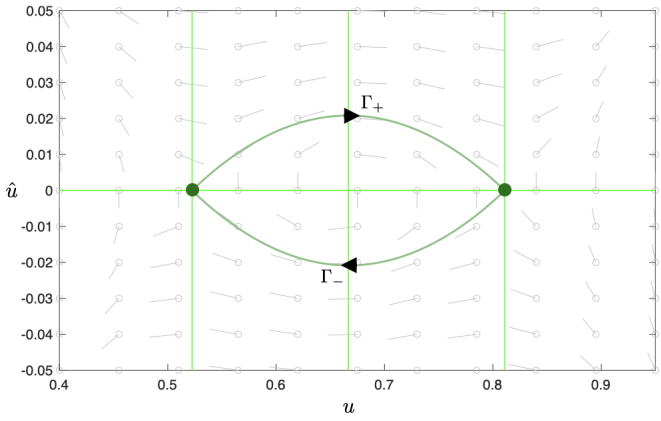

Figure 3: two heteroclinics $\Gamma_+ : p_l \to p_r$ and $\Gamma_- : p_r \to p_l$ for $\delta = 0$ and $w = w_h \approx -0.5648$ in $(u, \hat{u})$-space; other parameter values: $\beta = 6$, $\gamma_1 = 7/12$, $\gamma_2 = 3/4$.

3.1.2 The small $|\delta|$ case

For sufficiently small $|\delta| > 0$, we show that nearby heteroclinic connections to the same asymptotic end states still exist. This is done via a *Melnikov-type* argument; see, e.g., [24, 25]:

Define $x = (u, \hat{u})^\top$ and $f(x; w, \delta) = (\hat{u}, w + \Phi(u) - \delta\hat{u})^\top$ such that the layer problem is given in vector form by

$$x' = f(x; w, \delta)\,, \qquad x \in \mathbb{R}^2\,.$$

This system possesses heteroclinic orbits $\Gamma_\pm(y)$ for $w = w_h$ and $\delta = 0$, i.e., $\Gamma' = f(\Gamma_\pm; w_h, 0)$. Let $x = \Gamma_\pm + X$, $X \in \mathbb{R}^2$ which transforms the layer problem to the non-autonomous problem

$$X' = A(y)X + g(X, y; w, \delta)$$

with the non-autonomous matrix $A(y) := D_x f(\Gamma_\pm; w_h, 0)$ and the nonlinear remainder $g(X, y; w, \delta) = f(\Gamma_\pm + X; w, \delta) - f(\Gamma_\pm; w_h, 0) - A(y)X$. The linear equation

$$X' = A(y)X$$

is the *variational equation* along $\Gamma_\pm$. The corresponding *adjoint equation* is given by

$$\Psi' + A^\top(y)\Psi = 0\,.$$

Solutions of the variational and its adjoint equation preserve a constant angle along $\Gamma_\pm$, i.e., $D_y(\Psi^\top(y)X(y)) = 0, \forall y \in \mathbb{R}$. We can use this fact to define a splitting of the vector space $\mathbb{R}^2$ along $\Gamma_\pm$. Without loss of generality, we define it at $y = 0$ in the following way:

$$\mathbb{R}^2 = \text{span}\,\{f(\Gamma_\pm(0); w_h, 0)\} \oplus W$$

where W is spanned by the solutions of the adjoint equation that decay exponentially for $y \to \pm\infty$; here, this space is one-dimensional and we denote the corresponding solution by $\psi(y) = (\psi_1(y), \psi_2(y))^\top$.

We measure the distance $\Delta \in \mathbb{R}$ between the one-dimensional stable and unstable manifolds emanating from the saddle-equilibria in a suitable cross section Σ. We denote these manifold segments by $X_\pm$. Based on our setup, we choose $\Sigma = W$. This distance function depends on the system parameters, i.e., $\Delta = \Delta(w, \delta)$. In the previous section, we established $\Delta(w_h, 0) = 0$. Melnikov theory establishes the following distance function formula:

$$\begin{aligned}\Delta(w,\delta) &= \int_{-\infty}^{0} (\psi(s)^\top g(X_-(w,\delta)(y), y; w, \delta))ds - \int_{\infty}^{0} (\psi(s)^\top g(X_+(w,\delta)(y), y; w, \delta))ds\,, \\ &= \int_{-\infty}^{\infty} (\psi(s)^\top g(X(w,\delta)(y), y; w, \delta))ds\end{aligned} \tag{18}$$

where $X_\pm(w, \delta)(y)$ denotes the corresponding (un)stable manifold segments of the saddle equilibria $p_{l/r}$ from the corresponding saddle equilibrium to the cross section Σ, and X is the representative of these sets in the relevant domain.

Remark 3.3 *The distance function Δ is well-defined since $\psi(y)$ decays exponentially in forward and backward time and $X_\pm$ is bounded. The saddle equilibria $p_{l/r} = p_{l/r}(w, \delta)$ are robust under small perturbations (because they are hyperbolic) which guarantees the existence of these (un)stable invariant manifold segments nearby.*

In general, one cannot solve $\Delta(w, \delta) = 0$ explicitly. Thus one aims to solve $\Delta(w, \delta) = 0$ near $(w, \delta) = (w_h, 0)$ approximately by means of the implicit function theorem: e.g., if $D_w\Delta(w_h, 0) \neq 0$ then $w = w_h(\delta) = w_h + b\delta + O(\delta^2)$ solves $\Delta(w_h(\delta), \delta) = 0$ for $\delta \in (-\delta_0, +\delta_0)$. The leading order expansion parameter b is then given by

$$b = -\frac{D_\delta \Delta(w_h, 0)}{D_w \Delta(w_h, 0)}\,.$$

These first-order expansion terms of the distance function Δ are known as first-order *Melnikov integrals*, and they can be calculated as follows:

$$(D_w\Delta(w_h,0), D_\delta\Delta(w_h,0)) = (\int_{-\infty}^{\infty} (\psi(s)^\top D_w f(\Gamma_\pm(0); w_h, 0))ds,\ \int_{-\infty}^{\infty} (\psi(s)^\top D_\delta f(\Gamma_\pm(0); w_h, 0))ds)$$

We have $D_w f(\Gamma_\pm(0); w_h, 0) = (0, 1)^\top$ and, hence,

$$D_w\Delta(w_h,0) = \int_{-\infty}^{\infty} (\psi(s)^\top D_w f(\Gamma_\pm(0); w_h, 0))ds = \int_{-\infty}^{\infty} \psi_2(s)ds \neq 0,$$

based on the geometric observation that the ψ_2-component does not change sign along $\Gamma_\pm$. The integral is well-defined since $\psi_2(y)$ is decaying exponentially for $y \to \pm\infty$. Hence, $w = w_h(\delta) = w_h + b\delta + O(\delta^2)$ solves $\Delta(w(\delta), \delta) = 0$ for $\delta \in (-\delta_0, +\delta_0)$. We also have $D_\delta f(\Gamma_\pm(0); w_h, 0) = (0, -\hat{u}(y))^\top$ and, hence,

$$D_\delta\Delta(w_h,0) = \int_{-\infty}^{\infty} (\psi(s)^\top D_\delta f(\Gamma_\pm(0); w_h, 0))ds = -\int_{-\infty}^{\infty} \hat{u}(s)\psi_2(s)ds \neq 0\,,$$

based on a similar geometric observation as above, i.e., both terms do not change sign under the variation along $\Gamma_\pm$. Hence,

$$b = \frac{D_\delta\Delta(w_h,0)}{D_w\Delta(w_h,0)} = -\frac{\int_{-\infty}^{\infty} \hat{u}(s)\psi_2(s)ds}{\int_{-\infty}^{\infty} \psi_2(s)ds} \neq 0$$

and we have a leading order affine solution $w(\delta)$ to $\Delta(w, \delta) = 0$ near $(w_h, 0)$.

Remark 3.4 *Only for $(w, \delta) = (w_h, 0)$ does there exist two heteroclinics $\Gamma_\pm$ simultaneously. For fixed small $\delta \neq 0$, the two heteroclinics exist for distinct w-values. There is also the symmetry $\delta \leftrightarrow -\delta$. Thus one only needs to continue one heteroclinic in (w, δ)-space. The other is given through the symmetry.*

Remark 3.5 *The leading order linear growth found in the Melnikov analysis cannot continue indefinitely since the saddle equilibria $p_{l/r}$ are confined to w-values between the local extrema of Φ; see Remark 3.1. These extrema indicate saddle-node bifurcations of equilibria.*

3.1.3 The $\delta = O(1)$ case

In this section, we track the fate of the heteroclinic branches established in the previous section: do they exist for large $|\delta|$ as well? The layer flow confines any heteroclinic orbits connecting the outer two saddle points to live in the upper (Γ_+) or lower (Γ_+) half-plane in $(u, \hat{u})$-space. In these half-planes, the u-motion is monotone. Hence, all heteroclinics $\Gamma_\pm$ are graphs over the u-coordinate chart in $(u, \hat{u})$-space, i.e., $\Gamma_\pm : \hat{u}(u) : u \in (u_l, u_r)$. We consider Γ_+. Such a heteroclinic orbit $\hat{u}(u)$ must fulfill

$$\begin{aligned} & \frac{d\hat{u}}{du} = \frac{w + \Phi(u) - \delta\hat{u}}{\hat{u}}\,, \quad \forall u \in (u_l, u_r) \\ \Longrightarrow\ & \frac{d}{du}(\frac{\hat{u}^2}{2}) = \frac{d}{du}\int (w + \Phi(u) - \delta\hat{u})du\,, \quad \forall u \in (u_l, u_r) \\ \Longrightarrow\ & \frac{\hat{u}^2}{2} = \int_{u_l}^{u} (w + \Phi(u) - \delta\hat{u})du\,, \quad \forall u \in (u_l, u_r)\,. \end{aligned}$$

For $u \to u_l$, the last line is fulfilled since $\hat{u}(u_l) = 0$. For $u \to u_r$, where $\hat{u}(u_r) = 0$, we obtain a condition for the existence of a heteroclinic orbit,

$$\boxed{\int_{u_l}^{u_r} (w + \Phi(u))du = \delta \int_{u_l}^{u_r} \hat{u}(u)\, du\,,} \tag{19}$$

which, for $\delta = 0$, gives the equal area rule as established previously. For $\delta \neq 0$ this formula provides a generalised 'equal area rule', i.e., the left hand side must move away from its 'equal area' position given for $w = w_h(0)$ to counteract the right hand side contribution. This gives $w = w_h(\delta)$.
For sufficiently large $|\delta| = \delta_m$, w will reach its limit w_{sn} where one of the saddle equilibria $p_{l/r}$ goes through a saddle-node bifurcation. Until then, the heteroclinic connection is along the hyperbolic direction, but afterwards it will be along the centre direction which is non-unique and, hence, replaces the codimension-one role of the w variation. Hence, for fixed $w = w_{sn}$ and for sufficiently large $|\delta| > \delta_m$, there always exists a heteroclinic orbit.

Remark 3.6 *For $w = w_{sn}$, the rhs of (19) is fixed. One concludes that for sufficiently large $|\delta| > \delta_m$, there is a $\hat{u}(u)$ that fulfills the generalised equal are rule, i.e., that fixes the right hand side $\delta \int \hat{u}\, du$ to the correct value.*

Figure 5 summarizes our results on the existence of shocks in the regularised RND model, i.e., the solution branches of $\Delta(w, \delta) = 0$. The important insight here is that viscous relaxation is the dominant regularising effect for $|\delta| > |\delta_m|$

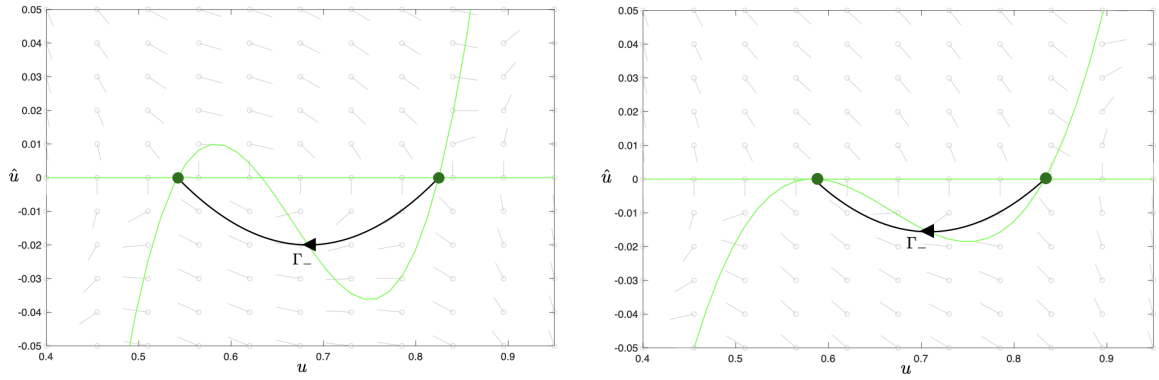

Figure 4: (left) heteroclinic Γ_- for $\delta = 0.1$ and $w = w_h(\delta) \approx -0.5661$, (right) border case heteroclinic Γ_- for $\delta = \delta_m \approx 0.248$ and $w = w_{sn} \approx -0.5671$; other parameter values: $\beta = 6$, $\gamma_1 = 7/12$, $\gamma_2 = 3/4$.

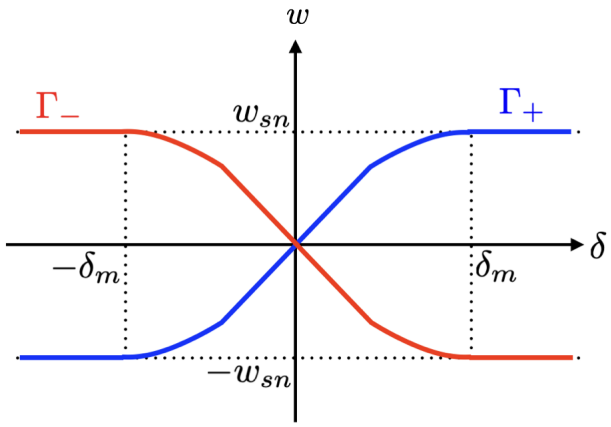

Figure 5: Sketch of complete bifurcation diagram for heteroclinic connections $\Gamma_\pm$ in (δ, w)-space centered at $(w_h(0), 0)$.

3.2 The limit on the slow scale - the reduced problem

For the slow system (9), the limit $\varepsilon \to 0$ gives the *reduced problem*

$$\begin{aligned} 0 &= \hat{u} \\ 0 &= w + \Phi(u) - \delta\hat{u} \\ v_z &= f(u) \\ w_z &= v + cu\,. \end{aligned} \tag{20}$$

It describes the 'evolution' of the slow variables (v, w) constrained to the 2D critical manifold S (12). Here, the critical manifold S is given as a graph over the (u, v)-space, i.e., $S : \psi(u, v) \in \mathbb{R}^4$. Therefore, we aim to study the corresponding reduced flow on S in this (u, v)-coordinate chart. By definition, the main requirement on the reduced vector field $R(u, v) \in \mathbb{R}^2$ is that, when mapped onto S via $D\psi$ it has to correspond to the (leading order) slow component of the full four-dimensional

vector field constraint to S, i.e.,

$$D\psi(u,v)R(u,v) = \Pi^S G(\psi(u,v)) = (\frac{v+cu}{-D(u)}, 0, f(u), v+cu)^\top$$

where $\Pi^S G(\psi(u,v))$ is the (oblique) projection of the vector field $G = (0,0,f(u),v+cu)^\top$ onto the tangent bundle TS of the critical manifold S along fast fibres spanned by $\{(1,0,0,0)^\top, (0,1,0,0)^\top\}$. Thus the reduced vector field $R(u,v)$ in the (u,v)-coordinate chart is given by (3).

3.2.1 Folded singularities: equilibria of the desingularised problem located on a fold F that are, in general, not equilibria of the reduced problem

This auxiliary system defines another type of singularities for the reduced problem through $D(u) = 0$ which exist on the folds $F_{l/r}$ and are known as *folded singularities*. In our problem, these folded singularities are given by $v_{f,l/r} = -cu_{f,l/r}$ where $u_{f,l/r} = \gamma_1, \gamma_2$. The Jacobian of the desingularised problem evaluated at folded singularities (u_{fs}, v_{fs}) is given by

$$J = \begin{pmatrix} -c & -1 \\ D'(u_{f\pm})f(u_{f\pm}) & 0 \end{pmatrix}$$

which has tr $J = -c$, det $J = D'(u_{f\pm})f(u_{f\pm})$ and $\mathcal{D} = c^2 - 4D'(u_{f\pm})f(u_{f\pm})$. Hence we are dealing for det $J < 0$ with a folded saddle (FS), and for det $J > 0$ with a folded node (FN) or a folded focus (FF) depending on the discriminant $\mathcal{D}$ being positive or negative.

$\phi(u)$	$f(u)$	(u_{f-}, v_{f-})	(u_{f+}, v_{f+})
DAD	logistic	'stable' FN/FF	FS

Table 4: Type of folded singularities on critical manifold S, logistic case

$\phi(u)$	$f(u)$	folded singularity	$\alpha > \gamma$	$\beta < \alpha < \gamma$	$\alpha < \beta$
DAD	bistable	(u_{f-}, v_{f-})	FS	'stable' FN/FF	'stable' FN/FF
DAD	bistable	(u_{f+}, v_{f+})	'stable' FN/FF	'stable' FN/FF	FS

Table 5: Type of folded singularities on critical manifold S, bistable case.

3.3 Constructing heteroclinic orbits that model shock-fronted travelling waves

The shock-fronted travelling waves that we seek are found as heteroclinic orbits of (9) connecting the saddle equilibrium at $u = 0$ to the one at $u = 1$. From the point-of-view of GSPT, a key observation is that solutions of the (fast) layer problem (11) and the (slow) reduced problem (3) can be concatenated to form singular heteroclinic orbits. Under suitable genericity assumptions, heteroclinic orbits of the regularised system then arise as a codimension-one family of perturbations of the singular connection for $0 < \varepsilon \ll 1$. See [15] for details of this construction in the setting of both 'pure' viscous relaxation and 'pure' nonlocal regularisation (5) resp. (6).

Here we extend this analysis to the case of nontrivial weightings of these two regularisations. In this section we use the parameter set $\beta = 6$, $\gamma_1 = 7/12$, $\gamma_2 = 3/4$, $\kappa = 5$, $\alpha = 1/5$ in order to depict

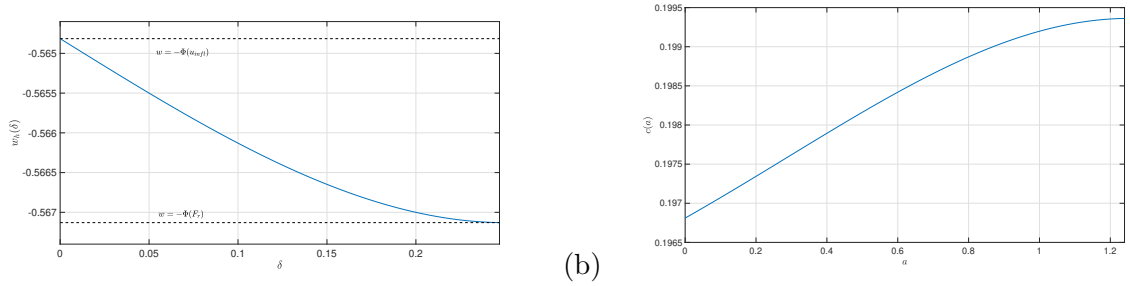

Figure 6: (a) Bifurcation diagram in (δ, w)-space for the shock height selection in the layer problem, corresponding to a segment of the branch Γ_-, as shown in Fig. 5. Here, $\delta_m \approx 0.248$. (b) Bifurcation diagram in (a, c)-space for the singular heteroclinic orbits. Parameter set: $\beta = 6$, $\gamma_1 = 7/12$, $\gamma_2 = 3/4$, $\kappa = 5$, $\alpha = 1/5$.

specific examples; this set is also chosen in order to extend the results in [16, 17, 15]. According to the Melnikov analysis in the previous sections, we can find a curve $w = w_h(\delta)$ in (δ, w) space for which there exist singular fast fronts connecting the outer two branches of the critical manifold; see Fig. 6(a). Under δ-variation, the shock connection varies continuously between the height specified by $w = -\Phi(u_{infl})$, where u_{infl} denotes the inflection point of the cubic (corresponding to the equal area rule), and a height specified by $w = w_{sn} = -\Phi(F_{l,r})$, where $F_{l,r}$ denote the u-values of the fold points of the critical manifold .

Let us now fix a value of $a \geq 0$. Then as the wavespeed parameter c varies, the corresponding extreme values $u = u_L(c)$, $u_R(c)$ selected by the shock also vary continuously according to the height condition $w_h(\delta) = w_h(ac) = -\Phi(u)$ specified by the layer problem.

Varying c simultaneously varies the (un)stable manifolds of the saddle points in the reduced problem. Suppose that the stable manifold $W^s(u_0, c)$ of the saddle point at $u_0 = 0$ has its first intersection with the cross-section $\{u = u_L(c)\}$ at a point $p_0(c)$, and similarly that the unstable manifold $W^u(u_1, c)$ of the saddle point at $u_1 = 1$ has its first intersection the cross-section $\{u = u_R(c)\}$ at $p_1(c)$. Under variation of c we can then locate a locally unique value $c = c(a)$ at which the v-coordinates of $p_0(c)$ and $p_1(c)$ coincide; i.e. so that the shock simultaneously connects two slow trajectories that join the two saddle points.

Altogether, we have defined a bifurcation problem for the singular heteroclinic orbits (modeling invasion fronts when $c > 0$) with respect to the regularisation weighting parameter a; see Fig. 6(b) for the resulting bifurcation diagram for our example parameter set. Figure 7 depicts an example of a singular heteroclinic connection formed under variation of the wavespeed parameter for fixed $a > 0$. We emphasize that each such invasion shock front formed within the parameter interval $a \in [0, a_m]$, with $a_m \approx 1.2465$, satisfies a distinct generalised area rule! A fixed wavespeed $c_m \approx 0.1994$ is selected for each $a > a_m$, since this is the wavespeed at which the portions of the singular heteroclinic connection that lie on the critical manifold connect to a viscous shock at the fixed height specified by $w_h(\delta) = w_{sn} = -\Phi(u)$, which is in turn satisfied for each $\delta > \delta_m$ (as depicted in Fig. 5).

After checking standard transversality conditions with respect to slow invariant manifolds and fast

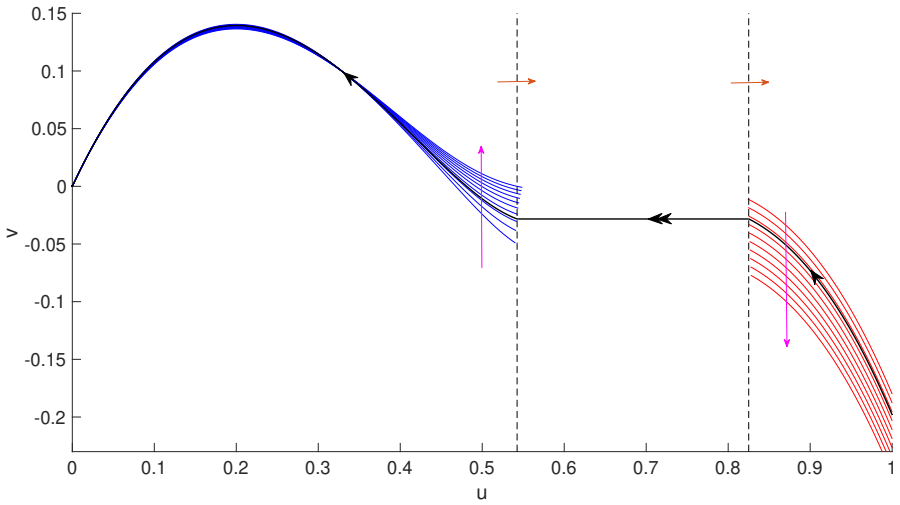

Figure 7: Singular heteroclinic orbit for $(a_*, c_*) \approx (0.5182, 0.19817)$, formed as a transversal intersection of the stable manifold $W^s(u_0, c)$ (blue curves) and unstable manifold $W^u(u_1, c)$ (red curves) as c is increased within the interval $[0.18, 0.25]$. Jump values $u = u_L(c_*)$, $u_R(c_*)$ satisfying $-w_h(\delta_* = a_* c_*) = \Phi(u)$ denoted by dashed black lines. Vertical magenta arrows: direction of variation of (un)stable manifolds; horizontal orange arrows: variation of the endpoints of the shock, as c increases. Parameter set: $\beta = 6$, $\gamma_1 = 7/12$, $\gamma_2 = 3/4$, $\kappa = 5$, $\alpha = 1/5$.

fibre bundles arising from Fenichel theory [4], and then applying well-known GSPT estimates (e.g. the Exchange Lemma), this family of singular heteroclinic orbits defined for $\varepsilon = 0$ generically perturbs to a codimension-one manifold of heteroclinic bifurcations of (10) in (a, c, ε) parameter space. An example of such an orbit, which satisfies a generalised area rule for a nontrivial value of $a > 0$, is depicted in Fig. 8.

4 Stability of shock-fronted travelling waves under composite regularisation

We now assess the stability of the travelling waves constructed in the previous section, with a focus on extending the analysis initiated in [16] and [17]. We adopt the standard approach of determining the spectral stability of the linearised operator L associated with the PDE (1), and linearised around a travelling wave. Our first step is to write down a suitable coordinate representation of L.

Let $\tilde{u}(z,t) = u(z) + \nu e^{\lambda t} p(z) + \mathcal{O}(\nu^2)$ denote a perturbation of a travelling wave $u(z)$ of (1), where λ is the temporal eigenvalue parameter and the variables in the linear term are assumed to separate. Inserting this solution into (1) and collecting terms of linear order in ν, we obtain the equation

$$(f'(u) - \lambda)p = -(cp + (D(u)p)_{zz} + \varepsilon a(\lambda p_{zz} - c p_{zzz}) - \varepsilon^2 p_{zzzz}). \tag{21}$$

Defining linearised variables $y := (p, q, r, s)$ corresponding to the nested derivatives on the right (analogously to what is done for the travelling wave system (9)), we arrive at the following nonau-

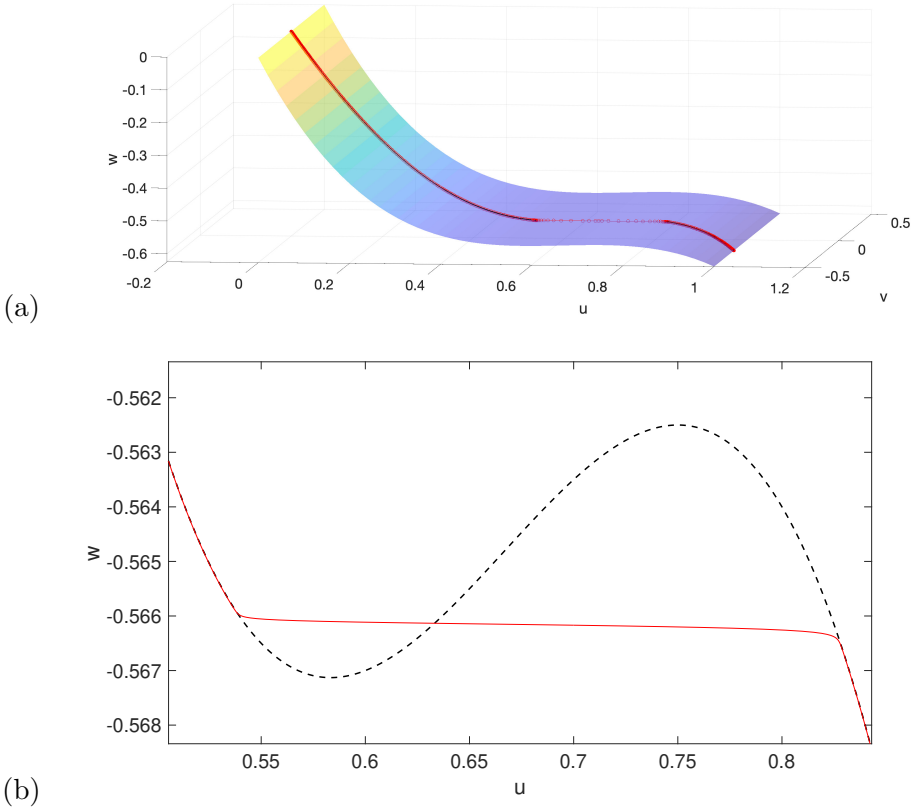

Figure 8: (a) A (u, v, w)-projection of a heteroclinic orbit of (10) for $\varepsilon = 10^{-4}$, $a \approx 0.5182$, and $c = 0.19826$. Black curve segments on the critical manifold (obscured by red curve) denote the slow portions of the corresponding singular heteroclinic orbit depicted in Fig. 7. (b) Side view of the heteroclinic orbit demonstrating that the connection satisfies the perturbed generalized area rule $w_h(\delta) = -\Phi(u)$. Parameter set: $\beta = 6$, $\gamma_1 = 7/12$, $\gamma_2 = 3/4$, $f_m = 5$, $\alpha = 1/5$. Computations performed with the `bvp4c` boundary value solver in MATLAB 2021a, with a relative error tolerance of 10^{-5}.

tonomous linear system:

$$\begin{aligned} \varepsilon \dot{p} &= q \\ \varepsilon \dot{q} &= (D(u) + \varepsilon a \lambda) p + s - \delta q \\ \dot{r} &= (f'(u) - \lambda) p \\ \dot{s} &= r + cp, \end{aligned} \tag{22}$$

or more compactly,

$$\dot{y} = M(z, \lambda, \varepsilon) y, \tag{23}$$

where $M(z, \lambda, \varepsilon)$ is a convenient matrix representation of L. We highlight the terms $\varepsilon a \lambda p$ and $-\delta q$ arising due to the viscous relaxation contribution.

By general theory (see e.g. [13]), the spectrum $\sigma(L)$ of L can be decomposed into its *point* and *essential* spectrum $\sigma(L) = \sigma_p(L) \cup \sigma_c(L)$. Our task is to ensure that the spectrum is bounded

within the left half complex plane, except for an eigenvalue at the origin that necessarily exists due to translational invariance. We must also check that the translational eigenvalue is simple.

4.1 Essential spectrum and sectoriality

We first give a brief overview of recent results for the essential spectrum. In [17], it was shown that for each $a \geq 0$, the essential spectrum is bounded well inside the left-half plane. To briefly summarise the approach, the *Fredholm borders* of $\sigma_e(L)$ are computed by tracking changes in the Fredholm index of the asymptotically constant matrices $M_\pm(\lambda, \varepsilon) := \lim_{z \to \pm\infty} M(z, \lambda, \varepsilon)$, which characterise the hyperbolic dynamics near the tails of the wave. We obtain the following parametrisations for the dispersion relations (with $k \in \mathbb{R}$):

$$\lambda_\pm(k) = \frac{f'(u_\pm) - D(u_\pm)k^2 - \varepsilon^2 k^4}{1 + a\varepsilon k^2} + ick. \tag{24}$$

We first verify that the essential spectrum lies entirely within the left half plane. This can be seen by noting that the denominator of the real part of $\lambda_\pm(k)$ in (24) is strictly positive, and then applying Descartes' rule of signs to the numerator, noting that $f'(u_\pm) < 0$, and $D(u_\pm)$ and ε are both positive. Since the numerator is an even polynomial, there are no real roots of the real part of $\lambda_\pm(k)$. Therefore, the essential spectrum is entirely contained in the left half plane.

Let us next recall that a linear operator L is *sectorial* if there exists $M > 0$ and $\eta < \pi/2$ such that $\lambda \notin \sigma(L)$ whenever $|\lambda| > M$ and $|\arg(\lambda)| < \pi - \eta$ (with $-\pi < \arg(\lambda) \leq \pi$) (see Prop 2.2 in [1]; see also Definition 1.3.1 in [9]). Sectoriality provides key resolvent estimates for the linearised operator: in particular, it allows us to conclude *nonlinear* stability from spectral stability, i.e. the existence of a neighborhood of initial conditions of the shock-fronted travelling wave tending to a translate of the wave exponentially quickly as time increases. Simultaneously, this property allows us to deduce the existence of a maximal compact contour K in the complex plane containing all of the point spectrum inside it.

We showed that the essential spectrum is asymptotically vertical (obstructing sectoriality) in the viscous relaxation limit (5) (see [17]), whereas the linearised operator *is* sectorial in the nonlocal limit (6) (see [16]). In this section, we demonstrate that sectoriality persists when $a > 0$. We follow the general approach of the proof of Prop 2.2 in Sec. 5B of [1]: we identify a suitable rescaling of the linearised variables in (22) in powers of $|\lambda|$, such that the $|\lambda| \to \infty$ limiting system takes an especially simple form. We use this simple form to determine that there is no unstable-to-stable connection made (i.e. there can be no spectrum for sufficiently large values of $|\lambda|$), as long as λ lies inside a suitable sector specified by the constraint on $\arg(\lambda)$.

It turns out that the appropriate choice of rescaling weights depends on whether $a = 0$ or $a > 0$. This dichotomy is not unexpected: for example, the asymptotic behaviour of the dispersion relations (24) is quite distinct in each case, with the relations flairing to the left with quartic growth when $a = 0$, but with only quadratic growth when $a > 0$.

We first consider the case $a = 0$, repeating the analysis in [16] but with a focus on rescaling the

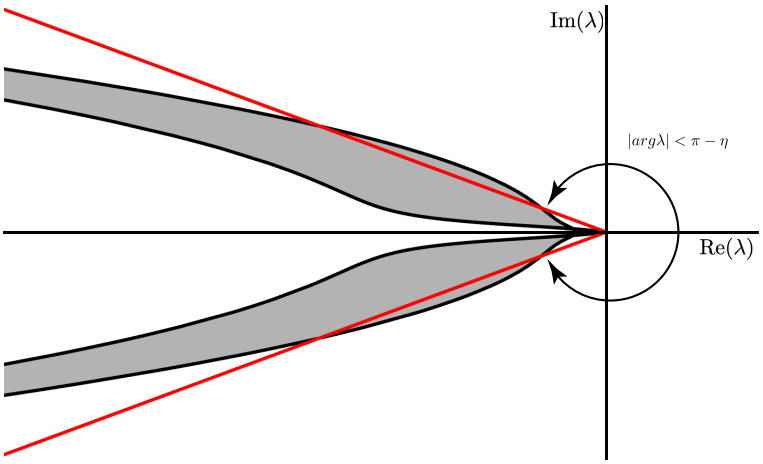

Figure 9: A schematic of the dispersion relations (black) from (24) enclosing the essential spectrum (grey), and an asymptotically bounding sector (red online). A bounding angle η is chosen such that the viscous relaxation contribution causes the dispersion relations to 'flair out' above the sector. The contributions from the Fourier transform of the nonlocal terms eventually take over for sufficiently large values of $|\lambda|$, and the dispersion relations return to being on the left of the bounding sector.

representation (22). Define the rescaled quantities

$$\tilde{p} = p, \quad \tilde{q} = q/|\lambda|^{1/4}, \quad \tilde{r} = r/|\lambda|^{3/4}, \quad \tilde{s} = s/|\lambda|^{1/2}, \quad \tilde{z} = z|\lambda|^{1/4}.$$

Writing the eigenvalue system (22) in terms of the rescaled variables $(\tilde{p}, \tilde{q}, \tilde{r}, \tilde{s})$ with rescaled 'time' $\tilde{z}$, and then taking the limit $|\lambda| \to \infty$, we find

$$\begin{aligned} \varepsilon \dot{\tilde{p}} &= \tilde{q} \\ \varepsilon \dot{\tilde{q}} &= \tilde{s} \\ \dot{\tilde{r}} &= -e^{i \arg \lambda} \tilde{p} \\ \dot{\tilde{s}} &= \tilde{r}. \end{aligned} \tag{25}$$

Remark 4.1 *The scaling weights n_p, n_q, ... in $\tilde{p} = p/|\lambda|^{n_p}$, $\tilde{q} = q/|\lambda|^{n_q}$, etc. can be chosen such that the limiting system* (25) *is autonomous and invertible, and so that the exponent of $|\lambda|$ balances to zero in the slow equation. This rescaling procedure can be interpreted geometrically as a Poincaré compactification of the vector field* (22) *'at infinity'; see e.g. [25].*

The eigenvalues of the linearisation of (25) are obtained from the roots of the quartic characteristic polynomial

$$e^{i \arg \lambda} + \varepsilon^2 \mu^4 = 0,$$

which can be solved explicitly to obtain the expressions

$$\mu = \frac{e^{i(\arg \lambda + m\pi)/4}}{\sqrt{\varepsilon}}, \quad m = 0,\ 1,\ 2,\ 3.$$

Note that this matches the 'large-scale' eigenvalues in [16] (c.f. eq. (20)), which were calculated using a different choice of rescaling weights. We point out that the asymptotic eigenvalue problem is independent of the wavespeed parameter.

Choose any $\eta \in (0, \pi/2)$. Then for each fixed $\varepsilon > 0$, two of these eigenvalues have strictly positive real part and the remaining two have strictly negative real part whenever $|\arg(\lambda)| < \pi - \eta$. Since (25) is autonomous, the corresponding unstable subbundle forms an attractor near to which solutions of the eigenvalue problem remain close by for all y, i.e. for sufficiently large $|\lambda|$ within the sector specified by the choice of η, there can be no contribution to the spectrum of the linearised operator. Furthermore, the eigenvalues remain well separated as $\varepsilon \to 0$.

Now we consider the case $a > 0$. In order to control the additional λ-dependent term in (22) when $|\lambda|$ grows large, we must also include $|\lambda|$ in the rescaling. We introduce an auxiliary rescaling parameter $\sigma > 0$ and write

$$\tilde{p} = p, \quad \tilde{q} = q\sigma, \quad \tilde{r} = r\sigma^3, \quad \tilde{s} = s\sigma^2, \quad \tilde{z} = z/\sigma, \quad |\lambda| = 1/\sigma^2.$$

With respect to this scaling, we have

$$\begin{aligned} \varepsilon\dot{\tilde{p}} &= \tilde{q} \\ \varepsilon\dot{\tilde{q}} &= \left(\sigma^2 D(u) + \varepsilon a e^{i\arg(\lambda)}\right)\tilde{p} + \tilde{s} - \sigma\delta\tilde{q} \\ \dot{\tilde{r}} &= (\sigma^4 f'(u) - \sigma^2 e^{i\arg(\lambda)})\tilde{p} \\ \dot{\tilde{s}} &= \tilde{r} + \sigma^3 c\tilde{p}. \end{aligned} \tag{26}$$

We are concerned with the dynamics near the limit $\sigma \to 0$. As in the purely nonlocal case, the limiting linear system has constant coefficients, but it is now *nonhyperbolic*:

$$\begin{aligned} \varepsilon\dot{\tilde{p}} &= \tilde{q} \\ \varepsilon\dot{\tilde{q}} &= \varepsilon a e^{i\arg\lambda}\tilde{p} + \tilde{s} \\ \dot{\tilde{r}} &= 0 \\ \dot{\tilde{s}} &= \tilde{r}, \end{aligned} \tag{27}$$

with eigenvalues

$$\mu = 0,\, 0,\, \pm\sqrt{\frac{a}{\varepsilon}}e^{i\arg(\lambda)/2}.$$

Thus, the analysis in this case is more delicate than in the previous case: we do not have access to an attractor (an unstable 2-plane bundle) in the large $|\lambda|$ limit, as one of the weak unstable directions degenerates to a center direction. We resort to standard perturbation theory. The eigenvalues of (26) can be determined to arbitrary order in σ (i.e. $1/|\lambda|$); we find that the pair of zero eigenvalues perturbs as

$$\mu = \pm\sqrt{\frac{1}{a\varepsilon}}\,\frac{1}{|\lambda|} + \mathcal{O}\left(\frac{1}{|\lambda|^2}\right).$$

We remind the reader that the system (26) is nonautonomous, but the relevant contributions from $D(u)$ and $f'(u)$ are bounded and do not affect the signs of the two smaller eigenvalues at leading

order. An invariant attractor over the unstable subbundle can be constructed explicitly by projectivizing the system and then using the theory of relatively invariant sets for nonautonomous systems (see Sec. B in [7]), but we avoid the detailed technicalities here. The argument for sectoriality in terms of bounding angles η then follows as in the purely nonlocal case. See Fig. 9 for a depiction of a bounding sector in relation to the essential spectrum.

We have shown that the appropriate cone estimate required for sectoriality holds for each $a \geq 0$, extending the result in [16]. This result has the following interesting implication: it is possible to retain sectoriality (and hence nonlinear stability) for travelling waves containing viscous shocks, when viscous relaxation is counterbalanced by nonlocal regularisation. We interpret this as reflecting the heuristic that 'pure' viscous relaxation is a somewhat degenerate regularisation, whereas nonlocal effects act as a generic perturbation.

4.2 Computation of the point spectrum

Let us fix the parameter set $\beta = 6$, $\gamma_1 = 7/12$, $\gamma_2 = 3/4$, $\kappa = 5$, $\alpha = 1/5$. In both the viscous relaxation limit (5) and the pure nonlocal regularization limit (6), there exist only two eigenvalues in the point spectrum for sufficiently small $\varepsilon > 0$: the simple translational eigenvalue $\lambda_0 = 0$, and another simple real eigenvalue $\lambda_1 \approx -0.8$ that does not affect the stability of the travelling wave (see [16, 17]). In this section we augment these results by sampling the point spectrum of the corresponding linearised operator for $\delta > 0$ and small values of $\varepsilon > 0$.

Let us outline the strategy to compute the point spectrum. For each $\lambda \in \mathbb{C}$ to the right of the essential spectrum, we can define an unstable complex 2-plane bundle $\varphi_+(z, \lambda, \varepsilon)$ extending from the unstable subspace of the saddle point at $u = 1$, resp. a stable complex 2-plane bundle $\varphi_-(z, \lambda, \varepsilon)$ extending from the stable subspace of the saddle point at $u = 0$, by using the eigenvalue problem (22). A (spatial) eigenvalue $\lambda \in \sigma_p(L)$ is found whenever φ_- and φ_+ have a nontrivial intersection at some value z; see [1] for details.

In view of this geometric characterization for the spatial eigenvalues, we will use a *Riccati-Evans function* to compute these intersections. The eigenvalue problem (22) induces a nonlinear flow on the Grassmannian $Gr(2, 4)$ of complex 2-planes in $\mathbb{C}^4$. On a suitable coordinate patch of $Gr(2, 4)$, the nonlinear flow is defined using a *matrix Riccati equation* of the form

$$W' = C + DW - WA - WBW, \tag{28}$$

where W is a complex-valued 2×2 matrix variable defined using frame coordinates for the 2-planes, and the 2×2 matrices A, B, C, D are defined via a block decomposition of the linear operator M in (23):

$$M = \left(\begin{array}{c|c} A & B \\ \hline C & D \end{array}\right). \tag{29}$$

See [8] and [14] for the derivation of (28), and [16] for the specific construction in the case of nonlocal regularisation (corresponding to $a = 0$ in (7)).

(a)

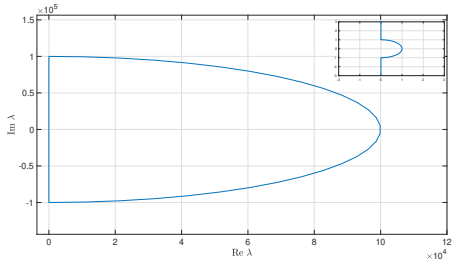

(b)

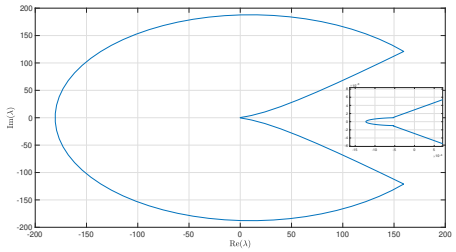

Figure 10: (a) Semicircular contour K of radius 10^5 along which the Riccati-Evans function (30) is evaluated. A small detour avoids the translational eigenvalue at the origin (inset). (b) Image $E(z_0, K)$ in the complex plane. Note that the image does not wind around the origin (inset). Parameter set as in Fig. 8.

In terms of the representation (30) of the projectivised dynamics, φ_+ is equivalent to the unique trajectory of (30) that converges to the unstable subspace of the saddle point at $u = 1$ as $z \to -\infty$; there is also an analogous characterisation of φ_-. We can now formulate a shooting problem defined on a suitable cross section that intersects the travelling wave transversely, say $\Sigma = \{u = 0.7\}$, with the corresponding intersection point z_0. The unstable bundle $\varphi_+(z, \lambda, \varepsilon)$ is flowed forward from $u = 1$ and the stable bundle $\varphi_-(z, \lambda, \varepsilon)$ is flowed backward from $u = 0$. The Riccati-Evans function $E(z_0, \lambda)$ is defined by

$$E(z_0, \lambda) = \det(\varphi_+(z_0, \lambda) - \varphi_-(z_0, \lambda)). \tag{30}$$

We can then find eigenvalues $\lambda \in \sigma_p(L)$ by locating zeroes of $E(z_0, \lambda)$; see [8]. Using the argument principle, we locate these zeroes by computing the winding number of E along suitably chosen contours in the complex plane and to the right of the essential spectrum.

We use a semicircular contour K with increasingly large radii $R = 10^3$, 10^4, 10^5 opening in the right half complex plane, with a small semicircular detour that avoids the translational eigenvalue at the origin (see Fig. 10(a)). We sampled the interval $[0, a_m]$ with a grid of 100 equally spaced points, and we fix $\varepsilon = 10^{-4}$. For each a in this sample, we evaluate $E(z_0, \lambda)$ around K to find a winding number of 0 (see e.g. Fig. 10(b)). Thus we obtain strong numerical evidence that there is no point spectrum within K, and hence that the corresponding family of shock-fronted travelling waves remains nonlinearly stable for each $a \in [0, a_m]$ and for each sufficiently small $\varepsilon > 0$.

We also investigated the zeroes of $E(z_0, \lambda)$ along the real line. For each sampled parameter value δ, we found evidence of only one simple translational eigenvalue $\lambda_0 = 0$ and one other simple real eigenvalue $\lambda_1 \approx -0.8$. We note that this result is entirely consistent with the calculation of the point spectrum in the 'purely nonlocal' and 'purely viscous' regularisation cases [16] and [17]; indeed, these eigenvalues are accounted for by the corresponding reduced *slow eigenvalue problem* defined on the critical manifold. As depicted in Fig. 6(b), singular heteroclinic connections are formed over a small range of wavespeeds $c \in [0.1973, 0.1993]$ as $a \geq 0$ is varied. This in turn slightly influences the dynamics of the reduced eigenvalue problem along the singular heteroclinic connection. As a consequence of these small variations, the (singular limit of the) secondary eigenvalue λ_1 moves continuously within the small interval $[-0.81, -0.79]$ on the real line as a is varied. The key point

that we would like to emphasize is that a slow eigenvalue problem (defined for $\varepsilon = 0$) continues to approximate the eigenvalues of the 'full' problem (defined for $0 < \varepsilon \ll 1$) when $a > 0$.

Remark 4.2 *It is interesting to ask whether the translational eigenvalue can bifurcate under variation of the regularisation parameter a via e.g. a transcritical crossing with the secondary eigenvalue $\lambda_1 = \lambda_1(a)$. In other words, is it possible to destabilize a (regularized) shock-fronted travelling wave of* (7) *just by re-weighting the regularization?*

We argue that such a destabilization scenario is not possible for families of monotone travelling waves. We showed using comparison methods in [17] that if a projectivized solution along a singular heteroclinic orbit of the reduced eigenvalue problem has no winds at $\lambda = \lambda_0 \in \mathbb{R}$, then no further winds are generated for each real $\lambda > \lambda_0$ (i.e. there are no more eigenvalues to the right of λ_0). Now suppose that the translational eigenvalue had a transcritical bifurcation for some critical value $a = a_c$ such that $\lambda_1(a) > 0$ for $a > a_c$. Then it must be true for nearby values of $a > a_c$ that the variational solution winds around at least once, i.e., the singular heteroclinic of (20) *in (u, v)-space makes a full revolution. But this is possible only if the wave is nonmonotone.*

Acknowledgement

This work has been funded by the Australian Research Council DP200102130 grant.

References

[1] J. Alexander, R. A. Gardner, and C. K. R. T. Jones. A topological invariant arising in the stability analysis of traveling waves. *J. Reine Angew. Math*, 410:167–212, 1990.

[2] K. Anguige and C. Schmeiser. A one-dimensional model of cell diffusion and aggregation, incorporating volume filling and cell-to-cell adhesion. *Journal of Mathematical Biology*, 58(3):395–427, jun 2008.

[3] J. W. Cahn. On spinoidal decomposition. *Acta. Metall.*, 9(795-801), 1961.

[4] N. Fenichel. Geometric singular perturbation theroy. *J Differential Equations*, 31:53–98, 1979.

[5] A. E. Fernando, K. A. Landman, and M. J. Simpson. Nonlinear diffusion and exclusion processes with contact interactions. *Physical Review E*, 81, January 2010.

[6] R. A. Fisher. The wave of advance of advantageous genes. *Annals of Eugenics*, 7:355–369, 1937.

[7] R. Gardner and C.K.R.T. Jones. Stability of travelling wave solutions of diffusive predator-prey systems. *Transactions of the AMS*, 327:465–524, 1991.

[8] K. E. Harley, P. van Heijster, R. Marangell, G. J. Pettet, T. V. Roberts, and M. Wechselberger. (in)stability of travelling waves in a model of haptotaxis. *submitted. 20 pages*, 2019.

[9] D. Henry. Geometric theory of semilinear parabolic equations. Number 840 in Lecture Notes in Mathematics. Springer–Verlag, New York, 1980.

[10] J. Hilliard. Spinodal decomposition. *in* phase transformations. *Am. Soc. Metals*, pages 497–560, 1970.

[11] S. T. Johnston, R. E. Baker, D. L. S. McElwain, and M. J. Simpson. Co-operation, competition and crowding: a discrete framework linking allee kinetics, nonlinear diffusion, shocks and sharp-frontec travelling waves. *Scientific Reports*, 7(42134), 2017.

[12] C. K. R. T. Jones. Geometric singular perturbation theory. *in Dynamical Systems, Springer Lecture Notes Math.*, 1609:44–120, 1995.

[13] T. Kapitula and B. Sandstede. Stability of bright solitary-wave solutions to perturbed nonlinear schrödinger equations. *Physica D: Nonlinear Phenomena*, 124(1):58–103, 1998.

[14] V. Ledoux, S. Malham, and V. Thümmler. Grassmannian spectral shooting. *Mathematics of Computation*, 79:1585–1619, 2010.

[15] Y. Li, P. van Heijster, M. J. Simpson, and M. Wechselberger. Shock-fronted travelling waves in a reaction–diffusion model with nonlinear forward–backward–forward diffusion. *Physica D*, 423(132916), 2021.

[16] I. Lizarraga and R. Marangell. Nonlocal stability of shock-fronted travelling waves under nonlocal regularization. *arXiv:2211.07824 (Preprint)*, 2022.

[17] I. Lizarraga and R. Marangell. Spectral stability of shock-fronted travelling waves under viscous relaxation. *arXiv:2208.10064 (Preprint)*, 2022.

[18] P. K. Maini, L. Malaguti, C. Marcelli, and S. Matucci. Aggregative movement and front propagation for bi-stable population models. *Mathematical Models and Methods in Applied Sciences*, 17(9):1351–1368, 2007.

[19] J.D. Murray. *Mathematical Biology I: An introduction*, volume 1 of *Interdisciplinary Applied Mathematics*. Springer, Hong Kong, 3rd edition, 2002.

[20] V. Padron. Effect of aggregation on population recovery modelled by a forward-backward pseudoparabolic equation. *Transactions of the American Mathematical Society*, 356(7):2739–2756, 2003.

[21] R. L. Pego. Front migration in the nonlinear Cahn–Hilliard equation. *Proc. R. Soc. Lond. A*, 422:261–278, 1989.

[22] C. J. Penington, B. D. Hughes, and K. A. Landman. Building macroscale models from microscale probablistic models: A general probablistic approach for nonlinear diffusion and multispecies phenomena. *Physical Review E*, 84, October 2011.

[23] P. Szmolyan and M. Wechselberger. Canards in $\mathbb{R}^3$. *J Differential Equations*, 177:419–453, 2001.

[24] A. Vanderbauwhede. Bifurcation of degenerate homoclinics. *Results in Mathematics*, 21(1-2):211–223, mar 1992.

[25] M. Wechselberger. Extending Melnikov theory to invariant manifolds on non-compact domains. *Dynamical Systems*, 17(3):215–233, aug 2002.

[26] M. Wechselberger and G. J. Pettet. Folds, canards and shocks in advection-reaction-diffusion models. *Nonlinearity*, 23:1949–1969, 2010.

[27] T.P. Witelski. The structure of internal layers for unstable nonlinear diffusion equations. *Studies in Applied Mathematics*, 96:277–300, 1996.